Dalton Transactions

Cite this: *Dalton Trans.*, 2012, **41**, 3536

www.rsc.org/dalton

PAPER

Super reduced Fe_4S_4 cluster of Balch's dithiolene series†

Ameerunisha Begum,* Golam Moula, Moumita Bose and Sabyasachi Sarkar*

Received 15th November 2011, Accepted 19th December 2011
DOI: 10.1039/c2dt12184k

A super reduced Fe_4S_4 cluster with a sulfur based radical, $[NBu_4]_4[Fe_3^{III}Fe^{II}(\mu_3\text{-}S)_4(mnt)_3^{6-}(mnt)^{1-\cdot}]^{4-\cdot}$, (**1**) (mnt, maleonitrile dithiolate) which evolves H_2S gas on treatment with acid under ambient conditions has been synthesized and structurally characterized. The Fe–S distances in **1** are in the range 2.246–2.383 Å, in stark contrast to that of the known $n = -2$ member of the series based on the $[Fe_4(\mu_3\text{-}S)_4(S_2C_2R_2)_4]^n$ unit (R = CF_3, Ph) with Fe–S bond lengths of 2.149–2.186 Å. The EPR of **1** displays very weak signals at *g*, 4.03 and 2.38 along with a strong S-based radical EPR signal at *g*, 2.003 associated with five structured components tentatively assigned to hyperfine interaction arising out of the naturally abundant ^{57}Fe with $\langle A \rangle = 88$ G. The EPR profile resembles the reduced Fe–S cluster of CO inhibited *Clostridium pasteurianum* W5 hydrogenase or the Fe_4S_4 centers of wild-type enzyme, *IspH* treated with HMBPP or IPP.

Introduction

The Fe–S clusters in hydrogenases shuttle electrons in catalyzing $H_2 \leftrightarrow 2H^+$ interconversion. [FeFe] hydrogenase from *Clostridium pasteurianum*, contains a $[Fe_4S_4]$ cubane sub-cluster covalently bridged by a cysteinate thiol to a [2Fe] sub-cluster, the center of action.[1] The $[Fe_4S_4]$ cubane sub-cluster transfers the electrons obtained from pyruvate oxidation to the [2Fe] sub-cluster.[2] The EPR spectrum with multiple hyperfine components of the hydrogenase of *Clostridium pasteurianum* W5 generated on exposure to CO could not be assigned to any particular ligand binding.[3] Similar EPR spectra have been recently reported for the Fe_4S_4 centers formed by the reduced, wild-type *Aquifex aeolicus* enzyme, *IsPH* [E-4-hydroxy-3-methyl-but-2-enyl diphosphate (HMBPP) reductase] and IPP (Isopentenyl diphosphate) or the wild-type enzyme plus HMBPP. The results indicated the involvement of an organometallic iron complex with HMBPP, a π/σ 'metallacycle' or η^2-alkenyl complex with iron–carbon (Fe–C) bonds, although there was no evidence for the formation of allyl radicals.[4]

Active site analogues of Fe–S proteins, *viz.*, $[Fe_4(\mu_3\text{-}S)_4(SR)_4]^{n-}$ were reported by Holm *et al.*[5] wherein these clusters contained peripheral ligands with monodentate thiolates and the Fe-sites were mostly of tetrahedral/pseudo tetrahedral nature. Fe_4S_4 cluster compounds bearing terminal bidentate thiolates with penta-coordinated Fe-sites have been comparatively less investigated and there is a single example in the five membered electron transfer related series ($n = 0, -1, -2, -3$ and -4) based on $[Fe_4(\mu_3\text{-}S)_4S_2C_2R_2)_4]^n$ (R = CF_3, Ph) unit with terminally coordinated 1,2-dithiolene ligands.[6–10] The Fe–S frameworks in $[Fe_4(\mu_3\text{-}S_4)(S_2C_2(CF_3)_2)_4]^n$ (n = 0, −2) are considerably stable and they undergo electron transfer reactions without a breakdown of the polynuclear skeleton. Dahl *et al.* reported that the replacement of the four terminal $S_2C_2(CF_3)_2$ ligands in the $[Fe_4(\mu_3\text{-}S)_4(S_2C_2(CF_3)_2)_4]^{2-}$ dianion with less π-acidic $S_2C_2(CN)_2$ ones should increase the Fe⋯Fe, S⋯S contacts and the Fe–S bond distances. Because of the air sensitivity, $n = -3$ and $n = -4$ members of the electron transfer series were not isolated.[11,12] 1,2-dithiolene coordinated metal complexes are known to undergo ligand centered oxidation/reduction involving dianionic to neutral to dipositive complexes and S-based radicals.[13–19] Radical based metal-dithiolate systems are expected to show unprecedented spectroscopic properties which are sometimes strikingly similar to that of the biological active sites.[20] Herein we report the synthesis of the hitherto unknown most reduced member of the electron transfer related series, $[NBu_4]_4[Fe_3^{III}Fe^{II}(\mu_3\text{-}S)_4(mnt)_3^{6-}(mnt)^{1-\cdot}]^{4-\cdot}$, (**1**) (mnt, maleonitrile dithiolate), its structure and unique EPR spectrum and its reactivity with weak acids.

Results and discussion

The complex **1** was synthesized by the reaction of $FeCl_3$ with disodium maleonitrile dithiolate and Li_2S in acetonitrile (CH_3CN) under Schlenk conditions and recrystallized from a mixture of CH_3CN and diethyl ether. Its crystals are composed of anions and tetrabutylammonium cations in a 1 : 4 ratio in the asymmetric unit. The perspective view of the anionic part of the complex **1** along with a tetrabutyl ammonium cation is displayed in Fig. 1 and selected crystal data are presented in Table 1. The crystal structure confirms the formation of tetrameric $[Fe_4(\mu_3\text{-}S)_4]$ cubane with terminal mnt coordination to the Fe centers. Six of the Fe–S distances are in range 2.246–2.276 Å whereas

---

Department of Chemistry, Indian Institute of Technology, Kanpur, Kanpur, 208016, India. E-mail: abya@iitk.ac.in; Fax: 915122597436; Tel: 91512 2597265

† CCDC reference number 788088. For crystallographic data in CIF or other electronic format see DOI: 10.1039/c2dt12184k

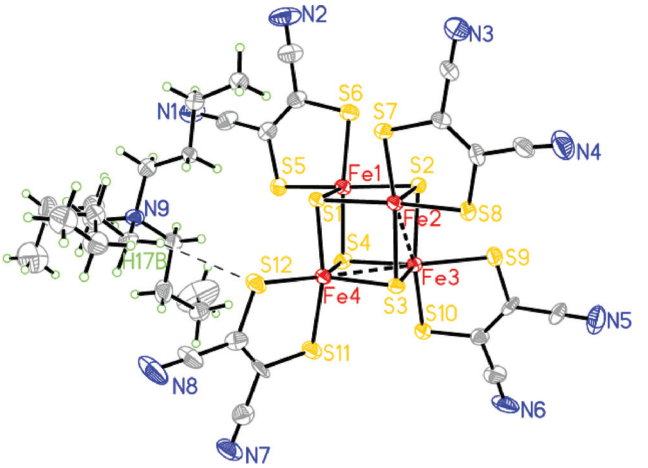

Fig. 1 A perspective view of the anionic part of complex **1** along with a tetrabutyl ammonium cation in 50% probability thermal ellipsoids. Selected bond lengths, (Å): Fe(1)–S(1), 2.297(3); Fe(1)–S(2), 2.256(3); Fe(1)–S(4), 2.256(3); Fe(1)–S(5), 2.265(3); Fe(1)–S(6), 2.264(3); Fe(2)–S(1), 2.233(3); Fe(2)–S(2), 2.260(3); Fe(2)–S(3), 2.310(3); Fe(2)–S(7), 2.263(3); Fe(2)–S(8), 2.265(3); Fe(3)–S(2); 2.305(3), Fe(3)–S(3); 2.252 (3); Fe(3)–S(4); 2.326(3), Fe(3)–S(9); 2.376(3); Fe(3)–S(10), 2.383(3); Fe(4)–S(1), 2.252(3); Fe(4)–S(3), 2.279(3); Fe(4)–S(4), 2.256(3); Fe(4)–S(11), 2.276(3); Fe(4)–S(12), 2.246(3); S(12)···H(17B), 2.93.

Table 1 Crystal data for (**1**)

Compound	(**1**)
Empirical formula	$C_{80}H_{144}Fe_4N_{12}S_{12}$
Formula weight	1882.19
T/K	120
Wavelength Mo-Kα (Å)	0.71073
Crystal system/Space group	Monoclinic/P_{21}/c
a/(Å)	30.853(7)
b/(Å)	11.326(2)
c/(Å)	31.285(7)
β/(°)	116.611(3)
Volume/Å^3/Z	9774(4)/4
Density (Mg m^{-3})	1.279
Absorption coefficient (mm^{-1})	0.883
F(000)	4016
θ range for data collection (°)	2.2 to 28.34
Unique reflections	23656
Observed reflections	8848
Completeness to $\theta = 26.00°$	97%
Absorption correction	Empirical
Data/restraints/parameters	23656/5/979
Goodness of fit on F^2	1.038
Final R_1 values [$I > 2\sigma(I)$]	0.1046
Final $wR(F^2)$ values [$I > 2\sigma(I)$]	0.2272

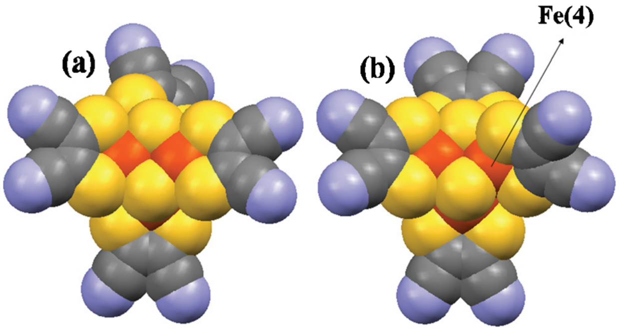

Fig. 2 The structure of the anionic part of **1** in a space filling model, (a) front view and (b) rear view. Note the distortion in the Fe(4) environment in part (b).

Table 2 C–S bond distances in **1** and in $[AsPh_4]_2[Fe_4(\mu_3\text{-}S)_4(S_2C_2(CF_3)_2)_4]$ (*ref. 11*)

Bond	**1** (Å)	(Ref. 11)^a (Å)
S(9)–C(9)	1.717(10)	1.66(3)
S(5)–C(1)	1.735(10)	1.69(3)
S(6)–C(2)	1.751(10)	1.70(3)
S(7)–C(5)	1.743(09)	1.74(3)
S(8)–C(6)	1.742(10)	1.75(3)
S(10)–C(10)	1.715(10)	1.69(3)
S(11)–C(13)	1.747(10)	1.75(4)
S(12)–C(14)	1.726(10)	1.76(3)

^{a} The atom numbers differ from those of **1**. (see Ref. 11).

the remaining two Fe–S bond distances are 2.376 and 2.383 Å. The Fe–S bond distances are considerably longer than those of the $n = -2$ member of the electron transfer series, $[Fe_4(\mu_3\text{-}S)_4S_2C_2(CF_3)_2)_4]^n$, *viz.*, Fe–S, 2.149–2.186 Å.[11] This might as well due to the coordination of CF_3 substituted dithiolene ligands. The Fe–Fe separations within the iron tetrahedron found in complex **1** (2.843–3.123 Å) are similar to those of the $n = -2$ member of the series and longer than those of the classical cubanes of Holm *et al.*[5,11] The S···S separations within the sulfur tetrahedron of **1** are longer than those of the Balch's complex $[Fe_4(\mu_3\text{-}S_4)(S_2C_2(CF_3)_2)_4]^{2-}$ and in the range 3.297–3.568 Å.

The notable feature in the structure of **1** is the considerably shorter C–S bond distances (C(9)–S(9), 1.716 Å and C(10)–S(10), 1.715 Å) of the mnt ligand coordinated to Fe(3) and the elongated Fe(3)–S bond distances. This is an indication of the oxidation of the ligand to its radical form and the possibility of the existence of the iron(II) oxidation state at this particular site (Fe(3)). It shows that there can be intramolecular electron transfer within the $\{Fe_4S_4\}$ core. 1,2-dithiolene metal complexes are known to undergo ligand centered oxidation/reduction involving dianionic to neutral to di-positive complexes and it is reflected in shortened C–S bond distances.[13–20] Within the $\{Fe_4(\mu\text{-}S)_4\}$ framework, although all of the four iron atoms are chemically identical, (all are coordinated to one terminal mnt ligand each) three of the Fe atoms (Fe(1)–Fe(3)) are in square pyramidal environments whereas the fourth Fe atom (Fe(4)) is severely distorted towards a trigonal bipyramidal structure, as shown in the space filling model (Fig. 2). Furthermore, intermolecular short contact between the mnt ligand attached to Fe(4) and the CH_2 group of the NBu_4 cations [(S(12)···H(17B), 2.93 Å] is also observed, which has been highlighted in Fig. 1.

The iron atom (Fe(3)), which is attached to the oxidized form of the terminal mnt ligands, is displaced as long as 0.629 Å, whereas the iron atoms Fe(1) and Fe(2) are displaced by 0.408 and 0.482 Å, respectively, from the basal plane formed by the S-donor atoms, and the geometry around Fe(4) is severely distorted towards a trigonal bipyramidal structure. In the $n =$

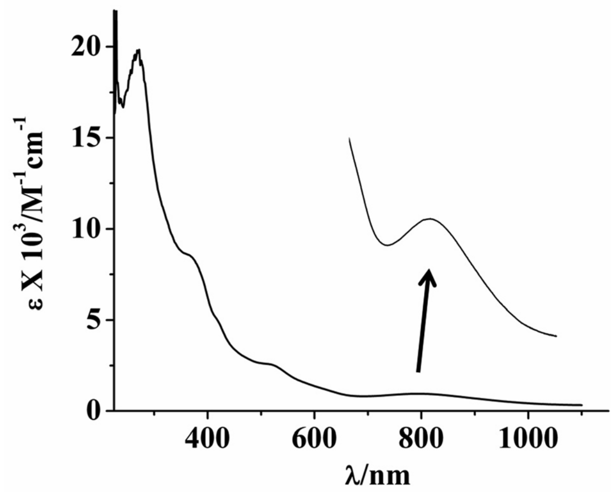

Fig. 3 The electronic spectrum of **1** in CH_3CN, (0.14 mM); inset is the visible spectrum showing the presence of the IVCT band in **1** around λ, 800 nm.

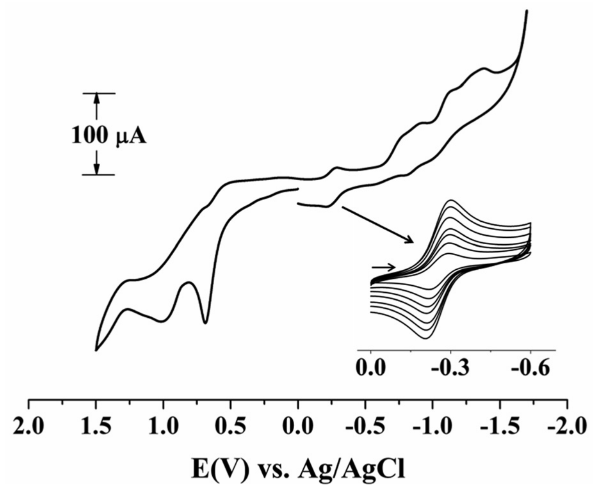

Fig. 4 A cyclic voltammogram of **1** (0.1 mM) in CH_3CN (supporting electrolyte, tetrabutylammonium perchlorate, 0.2 M); inset is the reversible redox couple at $E_{1/2}$, −0.258 V at different scan rates, 50 to 500 mV s^{-1}.

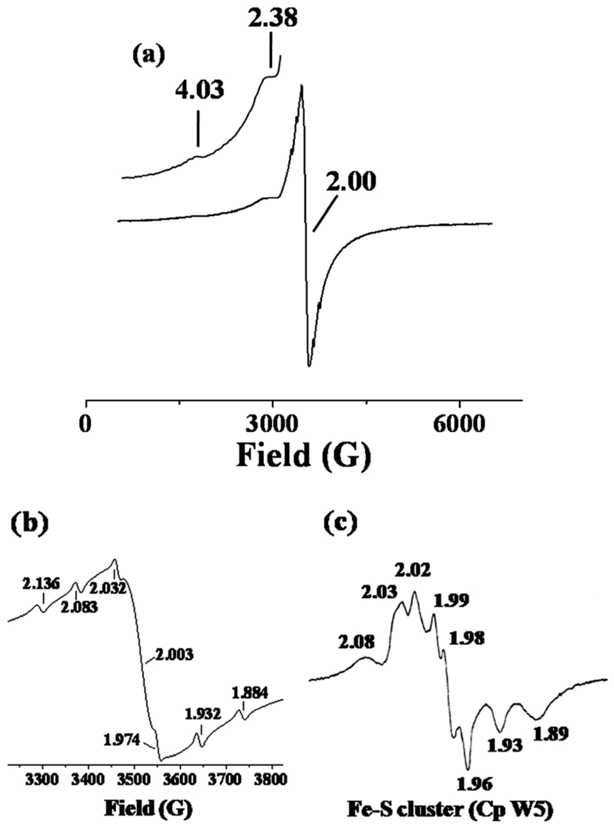

Fig. 5 (a) The X-band EPR of **1** at room temperature (298 K) in the range 0–6500 G with highlighted *g*-values on the top; (b) the X-band EPR of **1** in the range 3225–3825 G showing hyperfine structure and highlighted *g*-values on the top; (c) the EPR spectrum from Ref. 3.

−2 member[11] of the series *viz.*, $[Fe_4(\mu_3\text{-}S_4)(S_2C_2(CF_3)_2)_4]^{2-}$, the Fe atoms are displaced by 0.60 Å (average) above the basal sulfur plane and most of the C–S bond distances of dithiolene ligands are considerably shorter, *viz.*, C–S, 1.759, 1.753, 1,752, 1.739, 1.701, 1.693, 1.689, and 1.662 Å, as given in Table 2.

Complex **1** displays absorption bands around λ_{max} (ε), 800 nm (1000 $M^{-1}cm^{-1}$), 502 nm (2600 $M^{-1}cm^{-1}$), 361 nm (8600 $M^{-1}cm^{-1}$) and 270 nm (20 000 $M^{-1}cm^{-1}$) in CH_3CN (Fig. 3). All the three low energy bands in **1** are additional compared with 4-Fe and 8-Fe proteins' electronic signature known to be associated with the iron-sulfur chromophore.[5] The band around 800 nm in complex **1** can be assigned to an intervalence-charge transfer band (IVCT) which is observed in sulfur based radical containing complexes.[13–20] The cyclic voltammetric profile of complex **1** in CH_3CN (Fig. 4) displayed a reversible redox couple around $E_{1/2}$, −0.258 V and four irreversible reductions in the region, E_p, −0.770 to −1.380 V. The absorption band around $\lambda \sim 800$ nm and the reversible redox couple at $E_{1/2}$, −0.258 V (Fig. 4, inset) suggest the possibility of the presence of a ligand based radical which is corroborated by the X-ray structural parameters of the oxidized ligand *viz.*, the C–S bond distances (C(9)–S(9), 1.716 Å and C(10)–S(10), 1.715 Å) of the mnt ligand coordinated to the Fe(3) center.

However, the EPR measurement of complex **1** confirmed that it is paramagnetic and the solid state room temperature magnetic moment (μ_{eff}) of 2.8 μ_B is indicative of the presence of two odd electrons in the system. This can result from the presence of three S^{2-} bridged ferric ions of intermediate spins (s = 3/2) and one ferrous ion of low spin along with one mnt ligand based S-radical (s = 1/2) attached to the ferrous ion, Fe(3) resulting in two net odd electrons. This might as well have happened as a result of an intramolecular charge transfer from the mnt ligand to the originally ferric center Fe(3) giving an mnt ligand based radical and ferrous(Fe(3)) center.

Whereas the Mossbauer spectra of the neutral and dianionic forms[6,11] displayed doublets of δ = 0.32 and 0.39 mm s^{-1} and ΔE = 1.68 and 1.64 mm s^{-1}, the spectrum of **1**, the most reduced form of the series (n = −4), displayed a doublet of δ = 0.24 mm s^{-1} and ΔE = 1.42 mm s^{-1}. The Mossbauer spectral data reflect the identical iron environment of all four irons in **1** as well as in the already known members of Balch series, which is contrary to the crystal structural and other spectroscopic data. Furthermore, the Mossbauer spectral parameters of the reported members[6,11] and complex **1** indicate that the four Fe centers present inside the [Fe_4S_4] unit can not be differentiated by Mossbauer spectrometry. The room temperature (298 K) solid state EPR spectrum of **1** displayed a strong signal with *g*, 2.003 at 298 K (Fig. 5a) along with very weak signals at *g*, 4.03 and 2.38 supporting the presence of intermediate spin ferric ions. Interestingly the strong EPR signal centering at *g*, 2.003 is flanked by well resolved fine structure at *g*, 2.136, 2.083, 2.032, 1.974, 1.932 and 1.882 with the hyperfine coupling constant $\langle A \rangle = 88$ G as shown in Fig. 5b. At low temperature (120 K), the intensity of the EPR signals increased considerably but the EPR spectrum remained almost identical.

The CO inhibited and reduced form of *Clostridium pasteurianum* W5 hydrogenase exposed to CO gas displayed an EPR spectrum with similar fine structure, as shown in Fig. 5c, which can not be assigned to any specific ligands, because when 90% enriched CO was used only broadening of lines in the EPR spectrum was observed, whereas the fine structure was identical to the naturally abundant ^{12}CO containing system.[3] A similar EPR spectrum has been reported for the [Fe_4S_4] center found in the product formed by wild-type *IsPH* plus IPP or HMBPP, which has been reported to be due to the formation of a unique organometallic iron center rather than due to an organic radical.[4] In the former case,[3] it is highly probable that CO binds at the four iron centers leading to the formation of penta-coordinated iron centers which might exhibit an EPR spectrum with such a hyperfine structure and $\langle A \rangle$ values. Thus electronically **1** may resemble this native reduced species under CO since all of its four iron centers are penta-coordinated. We ascribe the EPR signal exhibited by complex **1** to the S-based radical of the oxidized mnt ligand attached to the low spin ferrous ion, (Fe(3)). The hyperfine splitting observed is due to the interaction with the nuclear moment of the naturally occurring low abundant ^{57}Fe nuclei (4Fe) in **1**. The observation of such hyperfine interaction even with low natural abundance is possible. A super hyperfine interaction based on the low abundance of the naturally occurring ^{13}C nuclei in the paramagnetic ion, $Mo(CN)_8]^{3-}$ is known.[21–23]

Reaction of complex 1 with acids

[FeFe] hydrogenase from *Clostridium pasteurianum*, contains a [$Fe_4(\mu_3\text{-}S_4)$] cubane sub-cluster covalently bridged by a cysteinate to a [2Fe] sub-cluster. In this system, the [2Fe] sub-cluster is regarded as the center of action whereas the [$Fe_4(\mu_3\text{-}S_4)$] cubane sub-cluster is involved in the electron transfer which obtains electrons from pyruvate oxidation.[2] Electrochemical proton reduction catalyzed by the model compounds is one of the current methods of estimation of hydrogenase activity wherein the catalytic efficiency is correlated to the shift of the reduction/oxidation potentials positively towards zero volts (−0.41 V at pH 7.0).[20,24] Complex **1** was tested for its catalytic efficiency for electrochemical proton reduction in CH_3CN. Upon addition of a standard acid like *p*-toluene sulfonic acid, (TsOH) a reversible redox couple at $E_{1/2} \sim -0.00$ V was observed. Controlled potential analysis of complex **1** containing excess of TsOH at $E_{1/2} \sim -0.200$ V was conducted in CH_3CN and the GC analytical result of the gas evolved did not match with that of the standard H_2 gas value. Hence the gas evolved was analyzed chemically by inserting cotton soaked with lead(II) acetate onto the lid of the electrochemical cell. The black coloration of the soaked cotton confirmed the evolution of H_2S gas. Similarly, complex **1** evolves H_2S on treatment with dilute acetic acid under ambient conditions *i.e.*, without applying any elctrochemical potential. This is reasonable because complex **1** contains acid labile inorganic S^{2-} groups similar to ferredoxin type clusters which on protonation release H_2S gas.

Conclusions

In summary, the fully reduced cluster **1** of the Balch series which evolves H_2S gas on treatment with acid under ambient conditions has been synthesized and structurally characterized. This shows an interesting EPR spectrum that resembles that of CO inhibited *Clostridium pasteurianum* W5 hydrogenase. A comparative study of electronic spectroscopy and cyclic voltammetric properties of **1** reveals the presence of a sulfur based radical inside the [$Fe_4(\mu_3\text{-}S_4)$] cluster which is corroborated by the short C–S bond lengths [(S(9)–C(9), 1.717(10) Å and S(10)–C(10), 1.715(10) Å].

Experimental

Materials and methods

All solvents and chemicals were purchased from commercial sources. Disodium maleonitrile dithiolate was synthesized by a reported procedure.[25] The electronic absorption spectroscopic measurements were conducted on a Perkin–Elmer Lambda 35 spectrometer. Infrared spectra were measured on a Bruker Vertex 70 FT-IR spectrometer. X-band EPR spectral measurements were done using a Bruker EMX Spectrometer. Solution magnetic moment measurement was done by Evans' method in DMF on a JEOL DELTA2 NMR spectrometer (500 MHz). Vibrating sample magnetic moment measurement was conducted on a EV-7 VSM ADE-DMS-Magnetic instrument within the field range of −17500 to +17500 Oe at room temperature (294–300 K). The data were corrected for diamagnetism of the sample holder and diamagnetic corrections for complex **1** were deduced from Pascal's constants. Mossbauer spectra were recorded using a conventional constant acceleration Mossbauer spectrometer (Wissenscaftliche Electronik GmbH0) with ^{57}Co in Rh matrix as the Mossbauer source. Cyclic voltammetric studies were carried out at 298 K on a BASi Epsilon-EC Bioanalytical systems in CH_3CN. Glassy carbon working, platinum wire auxiliary and Ag/AgCl with 3.0 M KCl reference electrodes were used. Tetrabutylammonium perchlorate (TBAP) of 0.2 M concentration was used as supporting electrolyte in CH_3CN. The electrochemical proton reduction using complex **1** and TsOH was conducted as reported previously.[20,24]

Generation of H_2S gas. Complex **1** (2 mmol) was taken in a two necked round bottomed flask fitted with a pressure equalizing funnel and the other neck of the flask was connected to a sulfuric acid trap. The whole set up was purged with argon gas for

30 min and then dil. CH_3COOH was added which resulted in a moderate stream of gas bubbling. The gas was allowed to pass through a colourless cotton soaked with a solution of lead(II) acetate. The black coloration of the soaked cotton confirmed the evolution of H_2S gas.

X-ray crystallographic measurement of 1. Single crystals of complex **1** were isolated as $[NBu_4]_4[Fe_3^{III}Fe^{II}(\mu_3\text{-}S)_4(mnt)_3^{6-}(mnt)^{1-\cdot}]^{4-\cdot}$ from the walls of the reaction flask at 10 °C. Complex **1** is extremely air sensitive and good quality crystals were not obtained. A crystal of better quality was used for the intensity data collection at 100 K on a Bruker AXS Smart APEX CCD diffractometer with graphite monochromated Mo-Kα radiation (0.71073 Å). Data reduction and absorption corrections were done using the SAINTPLUS program package. The structure was solved by direct and conventional Fourier methods and refined on F^2 by the full-matrix least-squares technique using the SHELXTL program package[26] All non-hydrogen atoms were refined anisotropically, H atoms at idealized positions in riding mode. Selected crystallographic data of complex **1** are given in Table 1. Detailed crystallographic data for **1** have been deposited in the Cambridge Crystallographic data centre as no. CCDC 788088.† Copies of the data can be obtained free of charge on application to CCDC, 12 Union Road, Cambridge CB2 1EZ, UK (Fax: (+44)1223-336-033) or e-mail: deposit@ccdc.cam.ac.uk.

Synthesis of $[NBu_4]_4[Fe_3^{III}Fe^{II}(\mu_3\text{-}S)_4(mnt)_3^{6-}(mnt)^{1-\cdot}]^{4-\cdot}$ (1). The reaction was done under inert (Schlenk) conditions. Acetonitrile (40 ml) was purged with argon gas for 30 min and disodium maleonitrile dithiolate (0.372 g, 2 mmol) was added into it. The suspension was stirred for 20 min. followed by the addition of $FeCl_3$ (0.322 g, 2 mmol) and Li_2S (0.15 g, 3 mmol) under argon. The black colored reaction mixture was stirred for 8 h at room temperature and at the end tetrabutyl ammonium bromide (0.665 g, 2 mmol) was added to the reaction mixture. After a further 30 min, diethylether (100 ml) was added to the reaction mixture. The reaction flask was closed and allowed to stand at 10 °C for two days under argon to precipitate a dark brownish-black colored precipitate. This was filtered, washed with ether and stored under argon. (Yield, 0.7 g, 74%). Black single crystals suitable for X-ray diffraction were isolated from the walls of reaction flask. The crystals of **1** were extremely air sensitive and perfect elemental analytical data could not be obtained. Data for **1**: Elemental analysis (%) calculated for $C_{80}H_{144}Fe_4N_{12}S_{12}$, C, 51.05, H, 7.71, N, 8.93; Observed, C, 51.82, H, 7.16, N, 8.02. FT-IR (KBr disc, cm^{-1}): 3019(m), 2962 (m), 2197(m, ν_{CN}), 1487s(m), 1401(w), 1243(w), 1147(w), 1020 (s) 602(br.) (w, weak, m, medium, s, strong). UV-visible in CH_3CN [λ/nm (ε/$M^{-1}cm^{-1}$)]: 800 (1000), 502 (2500), 361 (8500), 270(19800). EPR, g, 4.03, 2.38, 2.146, 2.089, 2.035, 1.983, 1.930, 1.881. $\mu_{eff} = 2.8\ \mu_B$ at 300 K. $E_{1/2} = -0.258$ V *vs.* Ag/AgCl (ΔE = 80 mV); E_p^{red} (irreversible), −0.935, −1.136, −1.379 V *vs.* Ag/AgCl; E_p^{ox} (irreversible), +0.686, +1.012 V *vs.* Ag/AgCl in CH_3CN–0.2M TBA with a GC working electrode.

Acknowledgements

A. B. thanks the Department of Science & Technology, (DST), N. Delhi, India for the award of fast track scheme for young scientists. G. M. and M. B. thank the Council of Scientific and Industrial Research, N. Delhi for the award of doctoral fellowships.

Notes and references

1 J. W. Peters, W. N. Lawzilotta, B. J. Lemon and L. C. Seefeldt, *Science*, 1998, **282**, 1853.

2 M. W. W. Adams and E. I. Stiefel, *Science*, 1998, **282**, 1842.

3 D. L. Erbes, R. H. Burris and W. H. Orme-Johnson, *Proc. Natl. Acad. Sci. U. S. A.*, 1975, **72**, 4795.

4 W. Wang, K. Wang, Y.-L. Liu, J.-H No, J. Li, M. J. Nilges and E. Oldfield, *Proc. Natl. Acad. Sci. U. S. A.*, 2010, **107**, 4522.

5 T. Herskovitz, B. A. Averill, R. H. Holm, J. A Ibers, W. D. Phillips and J. F. Weiher, *Proc. Natl. Acad. Sci. U. S. A.*, 1972, **69**, 2437.

6 A. L. Balch, *J. Am. Chem. Soc.*, 1969, **91**, 6962.

7 A. L. Balch, F. Roehrscheid and R. H. Holm, *J. Am. Chem. Soc.*, 1965, **87**, 2301.

8 W. C. Hamilton and I. Bernal, *Inorg. Chem.*, 1967, **6**, 2003.

9 T. Birchall, N. N. Greenwood and J. A. McCleverty, *Nature*, 1967, **215**, 625.

10 R. Williams, E. Billig, J. H. Waters and H. B. Gray, *J. Am. Chem. Soc.*, 1966, **88**, 43.

11 T. H. Lemmen, J. A. Kocal, F. Yip-Kwai Lo, M. W. Chen and L. F. Dahl, *J. Am. Chem. Soc.*, 1981, **103**, 1932.

12 T. Toan, B. K. Teo, J. A. Ferguson, T. J. Meyer and L. F. Dahl, *J. Am. Chem. Soc.*, 1977, **99**, 408.

13 P. Ghosh, A. Begum, D. Herebian, E. Bothe, K. Hildenbrand, T. Weyhermuller and K. Wieghardt, *Angew. Chem., Int. Ed.*, 2003, **42**, 563.

14 K. Ray, T. Weyhermuller, F. Neese and K. Wieghardt, *Inorg. Chem.*, 2005, **44**, 5345.

15 I. Shupack, E. Billig, R. J. H. Clark, R. Williams and H. B Gray, *J. Am. Chem. Soc.*, 1964, **86**, 4594.

16 D. T. Sawyer, G. S. Srivatsa, M. E. Bodini, W. Schaefer and R. M. Wing, *J. Am. Chem. Soc.*, 1986, **108**, 936.

17 K. Ray, T. Weyhermuller, A. Goossens, M. W. J. Craje and K. Wieghardt, *Inorg. Chem.*, 2003, **42**, 4082.

18 R. K. Szilagyi, B. S. Lim, T. Glaser, R. H. Holm, B. Hedman, K. D. Hodson and E. I. Solomon, *J. Am. Chem. Soc.*, 2003, **125**, 9158.

19 R. Sarangi, S. D. George, D. J. Rudd, R. K. Szilagyi, X. Ribas, C. Rovira, M. Almeida, K. O. Hodgson, B. Hedman and E. I. Solomon, *J. Am. Chem. Soc.*, 2007, **129**, 2316.

20 A. Begum, G. Moula and S. Sarkar, *Chem.–Eur. J.*, 2010, **16**, 12324.

21 E. Gelerinter, N. V. Duffy, S. S. Yarish, W. Dietzsch and R. Kirmse, *Chem. Phys. Lett.*, 1991, **184**, 375.

22 G. Teschmit and R. Kirmse, *Inorg. Chem. Commun.*, 1999, **2**, 465.

23 R. Kirmse, S. Saluschke, E. Moeller, E. J. Reijerse, E. Gelerinter and N. V. Duffy, *Angew. Chem., Int. Ed. Engl.*, 1994, **33**, 1497.

24 A. Begum and S. Sarkar, *Eur. J. Inorg. Chem.*, 2012, 40.

25 E. I. Stiefel, L. E. Bennett, Z. Dori, T. H. Crawford, C. Simo and H. B. Gray, *Inorg. Chem.*, 1970, **9**, 281.

26 G. Sheldrick, *Acta. Cryst.*, 2008, **A64**, 112.